Acta Cryst. (1993). B**49**, 283–289

Crystal Structure of $[(C_2H_5)_3NCH_3]Cu_3Cl_7$: a New Structural Variant of the $CuCl_2$ Structure

BY SHERRIE WEISE AND ROGER D. WILLETT

Department of Chemistry, Washington State University, Pullman, Washington 99164, *USA*

(*Received* 25 *May* 1992; *accepted* 27 *August* 1992)

Abstract

Triethylmethylammonium heptachlorotricuprate, $[(C_2H_5)_3NCH_3]Cu_3Cl_7$, $M_r = 555.0$, triclinic, $P\bar{1}$, $a = 7.917\ (5)$, $b = 11.131\ (7)$, $c = 11.664\ (7)$ Å, $\alpha = 65.71\ (3)$, $\beta = 86.86\ (3)$, $\gamma = 73.28\ (3)°$, $V = 894.8\ (9)$ Å^3, $Z = 2$, $D_x = 2.060$ g cm^{-3}, Mo $K\alpha$, $\lambda = 0.71073$ Å, $\mu = 45.6$ cm^{-1}, $F(000) = 546$, $T = 293$ K, $wR = 0.0675$ for 1222 observed $[|F| > 3\sigma(F)]$ reflections and 164 parameters. The compound consists of two-dimensional anionic $(Cu_3Cl_7^-)_\infty$ sheets separated by the organic cations. The sheets are made up of alternating metal halide rows. One half of the rows are infinite bibridged $(CuCl_2)_\infty$ chains. Interspersed between these rows are rows of discreet bibridged $Cu_2Cl_6^{2-}$ dimers. Adjacent rows are linked by long semi-coordinate Cu···Cl bonds. Adjacent dimers along the rows are separated by holes corresponding to the absence of Cu_2Cl_2 units. The cations sit directly above and below these holes to compensate for the loss in charge, with the methyl groups pointed toward the holes. The anionic sheets can be viewed as being derived from the ferrodistortive layers found in the parent $CuCl_2$ structure. A discussion of structures related to the $CuCl_2$ structure is given, with emphasis on the role that the cations and additional ligands have in developing these structures.

Introduction

One of the basic structures in crystal chemistry is the hexagonal layered CdI_2 structure (Wells, 1984) typically found for many MX_2 compounds. In this structure, the large X anions form hexagonal layers and the M^{2+} cations occupy octahedral holes between alternating layers. With the presence of a Jahn–Teller active metal ion, such as Cr^{2+} or Cu^{2+}, a ferroelastic distortion leads to the $CuCl_2$ structure (Wells, 1947). Because of the distortion, the cation in this structure can now be described as having a square-planar coordination geometry and clearly discernible bibridged $(CuCl_2)_\infty$ chains exist. The parentage to the CdI_2 structure is maintained, however, with longer semi-coordinate metal–halide bonds formed between chains. In this manner, each metal ion completes its coordination sphere in which it assumes an elongated octahedral coordination geometry, the so-called 4 + 2 geometry.

Features of the $CuCl_2$ structure are often still discernible when complex salts of CuX_2 are formed and/or a ligand is introduced into the coordination sphere. One particularly ubiquitous series of compounds formed have stoichiometries $A_2Cu_nX_{2n+2}$, $ACu_nX_{2n+1}L$, or $Cu_nX_{2n}L_2$, where A is a monovalent cation and L is a monodentate ligand (Willett, Grigereit, Halvorson & Scott, 1987). Compounds where A is replaced by a divalent cation or L by a bidentate ligand are also known. These structures generally contain finite quasiplanar oligomers that are recognizable as fragments of the chains present in the $CuCl_2$ structure. The formation of semicoordinate bonds between oligomers leads to a rich body of stacking patterns (see Bond & Willett, 1989), many of which can be related more or less directly to the $CuCl_2$ structure type.

The $CuCl_2$-based structures are one of three main structure types assumed in the crystalline state by octahedral copper(II) halide complexes. The principal characteristic in the $CuCl_2$-based series, in addition to the ferrodistortive arrangement of the Jahn–Teller elongation, is the existence of edge-sharing octahedra. In $(RNH_3)_2CuX_4$ systems, an antiferrodistortive version of the layer perovskite structures is observed (Willett, 1964). The parent perovskite structures contain layers of corner-shared octahedra (Balz, 1953). The Jahn–Teller-induced elongations in the Cu^{II} salts lie roughly in the plane of the layers but undergo 90° rotations between adjacent Cu^{II} sites. A detailed analysis of the structural characteristics of this series of compounds has recently been given (Willett, Place & Middleton, 1988). Another, not quite so common, structural class consists of derivatives of the $CsNiCl_3$ structure type. This consists of chains of face-shared octahedra (Tischenko, 1955). The sequence of Jahn–Teller elongations within a chain can now take on a variety of patterns and, because these patterns are close in energy, phase transitions are frequently observed (Willett, Bond, Haije, Soonieus & Maaskant, 1988).

0108-7681/93/020283-07$06.00

At higher temperatures many of the phases appear to involve dynamic reorientation of the Jahn–Teller axes (Tanaka, Iio & Nagata, 1985).

In the following two sections of this paper we report on the structure of $[(C_2H_5)_3CH_3N]Cu_3Cl_7$, encountered in attempts to prepare analogs of the incommensurate-bearing structure $[(CH_3)_4N]_2CuCl_4$ (Gomes-Cuevas, Tello, Fernandez, Lopez-Echarri, Herreros & Couzi, 1983) and of the magnetically interesting system $[(C_2H_5)_4N]_4Cu_4Cl_{12}$ (Willett & Geiser, 1986). This represents a new variant of the $CuCl_2$ structure and leads to speculation that additional variants may exist. In the final section, a summary is given of the relation of the various observed structures to the parent $CuCl_2$ structure.

Experimental

The compound was prepared by dissolving $[(C_2H_5)_3NCH_3]Cl$ and $CuCl_2$ (in excess) in dilute HCl and evaporating at room temperature until nearly dry. The solid material was collected, redissolved in nitromethane and crystals grown by slow evaporation at room temperature. A flat red crystal with dimensions $0.40 \times 0.35 \times 0.20$ mm was selected for data collection on a Syntex $P2_1$ diffractometer upgraded to Nicolet *P3F* specifications and equipped with a graphite monochromator. Lattice constants were obtained from 25 reflections in the range $26 < 2\theta < 30°$. Data were collected with ω scans (0.9°); two check reflections monitored every 96 reflections (011 and 022) show no systematic variations; 2522 total reflections out to $2\theta = 45°$, 2316 unique with R(merge) = 0.0430; hkl ranges, $0 \le h \le 8$, $-11 \le k \le 11$, $-12 \le l \le 12$ (Campana, Shepard & Litchman, 1981). Empirical ψ-scan absorption corrections were applied with the assumption of an ellipsoidal shaped crystal (relative transmission factors range from 0.577 to 0.883).

The structure solution was obtained *via* the direct-methods routine *SOLV* in the *SHELXTL* crystallographic program package and refinement also used that set of programs (Sheldrick, 1985). A difference synthesis based on the Cu and Cl positions thus obtained yielded the N- and C-atom positions. H atoms were constrained to ideal positions (C—H and N—H = 0.96 Å) and assigned isotropic thermal parameters 1.2 times larger than the associated atoms. Refinement proceeded in a straightforward fashion.

The final refinement resulted in $R = 0.0599$ (3σ data set) and 0.1179 (all data), where $R = \sum||F_o| - |F_c||/|F_o|$ and $wR = 0.0675$ (3σ data set) and 0.0898 (all data), where $wR = [\sum w(|F_o| - |F_c|)^2/\sum w|F_o|^2]^{1/2}$, with $w^{-1} = \sigma^2(F) + 0.0016F^2$. The goodness of fit was 0.965, $|\Delta/\sigma| = 0.001$. The largest peak on the final difference map was 0.6 e Å^{-3} near Cl(1), while the most negative excursion was -0.7 e Å^{-3}. Extinction corrections were made, with an extinction parameter of $x = 0.00001$ (10). Atomic coordinates are listed in Table 1, and bond distances and angles are given in Table 2.*

Table 1. *Atomic coordinates* ($\times 10^4$) *and equivalent isotropic displacement coefficients* (Å$^2 \times 10^3$)

Equivalent isotropic U defined as one-third of the trace of the orthogonalized U_{ij} tensor.

	x	y	z	U_{eq}
Cu(1)	8600 (3)	1327 (2)	8770 (2)	39 (1)
Cl(1)	5989 (6)	2875 (4)	8693 (5)	51 (2)
Cl(2)	8755 (6)	2175 (5)	6661 (4)	55 (3)
Cl(3)	8817 (6)	395 (4)	10940 (4)	45 (2)
Cu(2)	10882 (3)	3571 (2)	6333 (2)	40 (1)
Cu(3)	13853 (3)	1399 (2)	8770 (2)	40 (1)
Cl(4)	10894 (7)	4212 (5)	4182 (4)	52 (2)
Cl(5)	11231 (6)	3132 (5)	8430 (4)	43 (2)
Cl(6)	13585 (6)	1936 (5)	6666 (4)	52 (2)
Cl(7)	13777 (6)	528 (4)	10923 (4)	40 (2)
N	6612 (21)	2768 (16)	2975 (14)	53 (8)
C(1)	5704 (34)	3494 (25)	3747 (21)	122 (18)
C(2)	5336 (39)	2630 (39)	2250 (37)	212 (39)
C(3)	3796 (30)	3613 (24)	1562 (22)	114 (18)
C(4)	7527 (52)	3635 (32)	2059 (36)	243 (31)
C(5)	9035 (34)	3299 (29)	1495 (31)	184 (33)
C(6)	7669 (56)	1422 (31)	3707 (25)	238 (32)
C(7)	7324 (27)	388 (23)	4830 (20)	90 (14)

Structure description

The structure consists of copper chloride layers lying parallel to the $10\bar{1}$ planes, as shown in Fig. 1. The structure of these layers is closely related to the layer structure present in $CuCl_2$. The latter is built up of infinite bibridged chains linked together by semicoordinate bonds. The Cu—Cl bond distances within the chains are approximately 2.30 Å, while the semicoordinate bond distances are roughly 3.0 Å. A similar set of $(CuCl_2)_\infty$ chains exist in the title compound, running parallel to the $1\bar{1}1$ direction. Two-thirds of the Cu^{II} ions lie in these chains, with the average Cu—Cl distance equal to 2.304 (10) Å. Atom labels are given in Fig. 2, with distances and angles in Table 2. This and the average bridging Cu—Cl—Cu angles of 93.8 (7)° agree reasonably well with the average values reported for four other compounds containing infinite bibridged $CuCl_2$ chains (Willett, 1988). Interspersed between these chains are sets of discrete quasiplanar $Cu_2Cl_6^{2-}$ anions. The Cu—Cl distances are now considerably shorter [Cu—Cl (average) 2.276 (17) Å]. As is normal (Willett, 1988),

* Tables of data-collection parameters, anisotropic thermal parameters, H-atom parameters, and the observed and calculated structure factors, as well as a stereoview of the unit cell, have been deposited with the British Library Document Supply Centre as Supplementary Publication No. SUP 55649 (17 pp.). Copies may be obtained through The Technical Editor, International Union of Crystallography, 5 Abbey Square, Chester CH1 2HU, England. [CIF reference: CD0089]

Table 2. *Bond distances* (Å) *and angles* (°)

Cu(1)—Cl(1)	2.258 (5)	Cu(1)—Cl(2)	2.254 (5)
Cu(1)—Cl(3)	2.302 (5)	Cu(1)—Cl(3*a*)	2.292 (4)
Cl(1)—Cu(3*a*)	2.651 (6)	Cl(2)—Cu(2)	2.519 (7)
Cl(3)—Cu(1*a*)	2.292 (4)	Cu(2)—Cl(4)	2.309 (5)
Cu(2)—Cl(5)	2.304 (5)	Cu(2)—Cl(6)	2.305 (5)
Cu(2)—Cl(4*a*)	2.303 (5)	Cu(3)—Cl(5)	2.312 (5)
Cu(3)—Cl(6)	2.280 (5)	Cu(3)—Cl(7)	2.294 (4)
Cu(3)—Cl(1*a*)	2.651 (6)	Cu(3)—Cl(7*a*)	2.318 (4)
Cl(4)—Cu(2*a*)	2.303 (5)	Cl(7)—Cu(3*b*)	2.318 (4)
N—C(1)	1.475 (34)	N—C(2)	1.431 (49)
N—C(4)	1.438 (41)	N—C(6)	1.406 (30)
C(2)—C(3)	1.395 (34)	C(2)—C(4)	2.276 (60)
C(2)—C(6)	2.267 (47)	C(4)—C(5)	1.363 (49)
C(6)—C(7)	1.420 (35)		

Cl(1)—Cu(1)—Cl(2)	94.6 (2)	Cl(1)—Cu(1)—Cl(3)	91.3 (2)
Cl(2)—Cu(1)—Cl(3)	172.9 (2)	Cl(1)—Cu(1)—Cl(3*a*)	173.8 (2)
Cl(2)—Cu(1)—Cl(3*a*)	91.2 (2)	Cl(3)—Cu(1)—Cl(3*a*)	83.0 (2)
Cu(1)—Cl(1)—Cu(3*a*)	98.8 (2)	Cu(1)—Cl(2)—Cu(2)	101.9 (2)
Cu(1)—Cl(3)—Cu(1*a*)	97.0 (2)	Cl(2)—Cu(2)—Cl(4)	94.8 (2)
Cl(2)—Cu(2)—Cl(5)	95.1 (2)	Cl(4)—Cu(2)—Cl(5)	170.1 (2)
Cl(2)—Cu(2)—Cl(6)	102.2 (2)	Cl(4)—Cu(2)—Cl(6)	91.3 (2)
Cl(5)—Cu(2)—Cl(6)	86.0 (2)	Cl(2)—Cu(2)—Cl(4*a*)	104.6 (2)
Cl(4)—Cu(2)—Cl(4*a*)	85.3 (2)	Cl(5)—Cu(2)—Cl(4*a*)	92.8 (2)
Cl(6)—Cu(2)—Cl(4*a*)	153.2 (2)	Cl(5)—Cu(3)—Cl(6)	86.4 (2)
Cl(5)—Cu(3)—Cl(7)	93.6 (2)	Cl(6)—Cu(3)—Cl(7)	167.3 (2)
Cl(5)—Cu(3)—Cl(1*a*)	96.7 (2)	Cl(6)—Cu(3)—Cl(1*a*)	98.3 (2)
Cl(7)—Cu(3)—Cl(1*a*)	94.3 (2)	Cl(5)—Cu(3)—Cl(7*a*)	171.4 (2)
Cl(6)—Cu(3)—Cl(7*a*)	91.2 (2)	Cl(7)—Cu(3)—Cl(7*a*)	87.0 (2)
Cl(1*a*)—Cu(3)—Cl(7*a*)	91.8 (2)	Cu(2)—Cl(4)—Cu(2*a*)	94.7 (2)
Cu(2)—Cl(5)—Cu(3)	93.3 (2)	Cu(2)—Cl(6)—Cu(3)	94.1 (2)
Cu(3)—Cl(7)—Cu(3*b*)	93.0 (2)	C(1)—N—C(2)	109.9 (21)
C(1)—N—C(4)	107.9 (24)	C(2)—N—C(4)	105.0 (25)
C(1)—N—C(6)	112.8 (18)	C(2)—N—C(6)	106.1 (27)
C(4)—N—C(6)	114.8 (24)	N—C(2)—C(3)	128.8 (37)
N—C(2)—C(4)	37.6 (15)	C(3)—C(2)—C(4)	110.1 (25)
N—C(2)—C(6)	36.6 (14)	C(3)—C(2)—C(6)	162.8 (37)
C(4)—C(2)—C(6)	63.7 (16)	N—C(4)—C(2)	37.4 (17)
N—C(4)—C(5)	130.3 (27)	C(2)—C(4)—C(5)	122.1 (33)
N—C(6)—C(2)	37.3 (18)	N—C(6)—C(7)	130.2 (31)
C(2)—C(6)—C(7)	114.6 (29)		

the terminal distances are considerably shorter [average 2.256 (6) Å] than the bridging distances [average 2.297 (7) Å]. The bridging Cu—Cl—Cu angle (of interest for magnetic properties) has the second largest value reported in $Cu_2Cl_6^{2-}$ species. The dimers are roughly coplanar with the $(CuCl_2)_\infty$ chains, with the long axis of the dimers lying parallel to the chain direction. Adjacent layers are separated from each other by the organic cations.

The dimers and chains are interlinked *via* semicoordinate bonds ranging from 2.519 (7) Å for Cu(2)—Cl(2) to 3.219 (5) Å for Cu(3)—Cl(3). Each Cu atom has a different coordination geometry defined because of the intricateness of these semicoordinate bonds. The $Cu_2Cl_6^{2-}$ anions are essentially planar and are located nearly equidistant between neighboring chains. The Cu(1) atoms thus have close to ideal 4+2 geometries, with semicoordinate distances of 3.080 (6) and 3.192 (6) Å. In the chain, Cu(2) is situated so that it forms only one semicoordinate bond, which is extremely short at 2.519 (7) Å. In fact, it is so short that the coordination geometry is best described as square pyramidal. This Cu atom lies significantly above the plane (0.366 Å) of the four basal Cl atoms, with *trans* Cl—Cu—Cl angles of 170.1 (2) and 153.2 (2)°. This imposes a distortion upon the chain structure, which is also reflected in the geometry about Cu(3). For this Cu atom, the coordination geometry is appropriately described as 4 + 1 + 1, with one short semicoordinate distance of 2.651 (6) Å and the second much longer at 3.219 (6) Å. The square-pyramidal parentage of this geometry is evident in the distortion of the basal plane, where the *trans* Cl—Cu—Cl angles are 167.3 (2) and 171.4 (2)°, with Cu(3) lying 0.211 Å out of the plane of the four basal Cl atoms.

From Fig. 1, it is observed that adjacent dimers are separated by 'holes' that prevent the completion of the $(CuCl_2)_\infty$ chain structure. These holes correspond to the absence of $Cu_2Cl_2^{2+}$ units. To compensate for this loss in charge, one cation sits above and another sits below each hole (only those 'below' the holes are shown in Fig. 1, to preserve the clarity of the layer structure). The methyl groups of the cations are directed towards the holes, which provides for the most effective charge compensation. It is this interaction that leads to the stability of the structure and to the unique derivative structure of the parent $CuCl_2$ structure type.

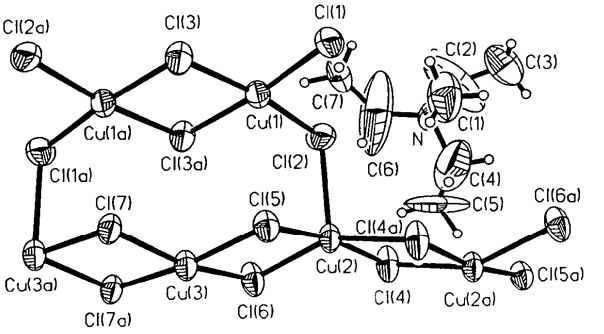

Fig. 1. Illustration of a portion of the structure, showing labeling scheme for the atoms.

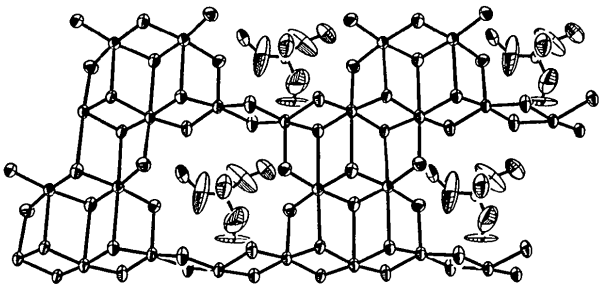

Fig. 2. Illustration of the layer structure, illustrating the relation of the cations to the holes in the layer. Cations on the near side of the layer are omitted for clarity.

Structure relationships

The central feature of the $CuCl_2$ structure type is the ferrodistortive nature of the Jahn–Teller-induced elongation of the Cu^{II} coordination geometry. This produces the clearly recognizable bibridged chain structure associated with that structure type. The presence of the semicoordinate bonds between chains preserves the layer structure of the parent CdI_2 structure, in contrast to the $PdCl_2$ structure (Wells, 1984). Many of the structures for more complex Cu^{II} halide salts and complexes retain a substantial portion of this ferrodistortive two-dimensional network.

In this section, a summary of the relationships of a number of the observed derivative structures will be given. A pictorial representation of the $CuCl_2$ structure is given in Fig. 3. Here the bibridged chains run horizontally. Semicoordinate linkages between chains are represented by dashed lines. Upon formation of a more complex structure, one or more things may happen, including fragmentation of the chains, insertion of stacking faults between chain fragments, removal of copper ions and insertion of ligands (or halide ions) between chains.

Termination of chains

Termination of the chains occurs when two halide ions and/or ligands are inserted at periodic intervals along the chains. Each insertion of a halide ion requires the inclusion of one monocation to maintain charge balance. This leads to the commonly observed compounds of stoichiometry $A_2Cu_nX_{2n+2}$, $ACu_nX_{2n+1}L$ or $Cu_nX_{2n}L_2$, where n commonly takes on values from 1 to 4, but examples with $n = 5$, 6 and 7 are also known (Willett & Rundle, 1964; Willett, Grigereit, Halvorson & Scott, 1987; Bond & Willett, 1989; Manfredini, Pellacani, Bonamartini-Corradi, Battaglia, Guarini, Giusti, Pon, Willett & West, 1990). A rich body of stacking patterns is associated with the formation of semicoordinate bonds between the oligomer units (Geiser, Willett, Lindbeck & Emerson, 1986; Willett, Bond & Pon, 1990). A subset of these structures corresponds to simple slabs of the $CuCl_2$ structure. Examples are illustrated in Fig. 4 for several $n = 3$ oligomers.

The envelope diagram representing each stacking pattern, as well as the Geiser notation for the stacking pattern, is given.* Which stacking pattern is preferable depends in some complex fashion upon the nature of the counterions and/or non-halide ligands. One would anticipate that the stacking patterns that maximize the number of semicoordinate bonds would be favored. In some cases, however, the most favorable packing appears to occur when the cation lies parallel to and directly on top of a portion of the oligomer. This is observed with *N*-methylated pyridinium cations (Bond, 1990; Bond, Place, Willett, Liu, Grigereit, Drumheller & Tuthill, 1993).

Termination of chains with stacking faults

The stacking patterns discussed above present only a small fraction of the patterns observed in Cu_nX_{2n+2}-type oligomers. In the parent CdI_2 structure, the metal ions occupy octahedral holes between alternate hexagonal layers of anions. The stacking faults correspond to a shift of a row of metal ions from sites between one pair of layers to sites between the adjacent pair of layers. In terms of the semicoordinate linkages between oligomers, these faults correspond to the alternation of the Cu···*X* linkages from one edge of the oligomer to the opposite edge of the oligomer. This leads to a variety of stacking patterns as illustrated in Fig. 5. The patterns are most clearly seen through the associated envelope diagrams. A phenomenological approach has been developed to predict additional types of stacking patterns, many of which exhibit these types of stacking faults (Willett, Bond & Pon, 1990). It is worthwhile noting that the stacking patterns given by the Geiser notation 1 $(\frac{1}{2}, \frac{1}{2})$, 1 $(\frac{1}{2}, \frac{1}{2})(\frac{1}{2}, -\frac{1}{2})$ and 1 $(\frac{1}{2}, \frac{1}{2})(-\frac{1}{2}, -\frac{1}{2})$ correspond to the Hatfield types I, II and III respectively (Hatfield, 1985).

A more drastic distortion of the structure, but one that still retains the ferrodistortive nature of the lattice, occurs in certain $A_2Cu_2X_6$ systems (Willett, 1966). Here the stacking 'faults' involve 90° rotations of the dimers about the normal to the dimer plane, as seen in Fig. 5(*d*).*

Removal of positive fragments from the $CuCl_2$ *layers*

In the above example, inclusion of cations in the structure was accompanied by the insertion of halide ions into the chain, forming oligomers of finite

* The general stacking pattern symbol, n $(m_{\|}, m_{\perp})$ is defined as follows: n is the number of Cu^{II} ions in the oligomer and $m_{\|}d$ and $m_{\perp}d$ are the translations parallel and perpendicular, respectively, to the Cu—Cu axis of the oligomer necessary to bring the centre of one oligomer on top of its neighbor in the stack (d is the ligand–ligand distance along the edge of the oligomer). As many sets of parenthetical quantities are concatenated as necessary so as to define the repeat pattern of the stacks.

* The rotations are included as part of the notation with the sense of the rotation (±) corresponding to anticlockwise or clockwise rotations.

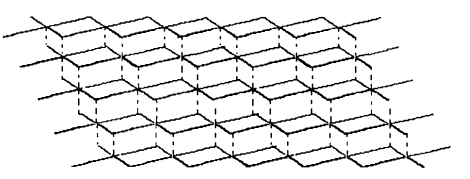

Fig. 3. Representation of the $CuCl_2$ structure.

length. One alternative method of keeping charge balance is to remove positive charge from the layer structure of parent $CuCl_2$ structures. In the title compound, this was accomplished by the removal of $Cu_2Cl_2^{2+}$ fragments periodically along alternating chains, as illustrated in Fig. 6(*a*). The charge balance is nicely accounted for by the clustering of two cations about the hole from which the fragment was removed. The periodicity, as well as the alternation of chains in which removal occurs, is certainly dictated by the size of the cation. A similar loss of $Cu_2Cl_2^{2+}$ fragments occurs in the $(Me_4P)Cu_2Cl_5$ (Haije, Dobbelaar & Maaskant, 1986) and $(Me_4As)Cu_2Cl_5$ (Murray & Willett, 1993) structures. However, the higher density of holes thus created leads to more severe distortions of the layers. In particular, the ferrodistortive nature of the distortions of the coordination geometries are lost and the coordination geometries are more appropriately described as square pyramidal. Alternative arrangements, such as the hypothetical $A_2Cu_3X_8$ and $A_2Cu_4X_{10}$ structures in Figs. 6(*b*) and 6(*c*) are possible. Removal of single Cu^{II} ions is energetically unfavorable. This would leave halide ions dangling on either side of the hole at distances much shorter than van der Waals contact distances (but see following section). Removal of larger fragments with higher charge would also be energetically unfavorable, since it is not possible to pack more than two cations about the hole.

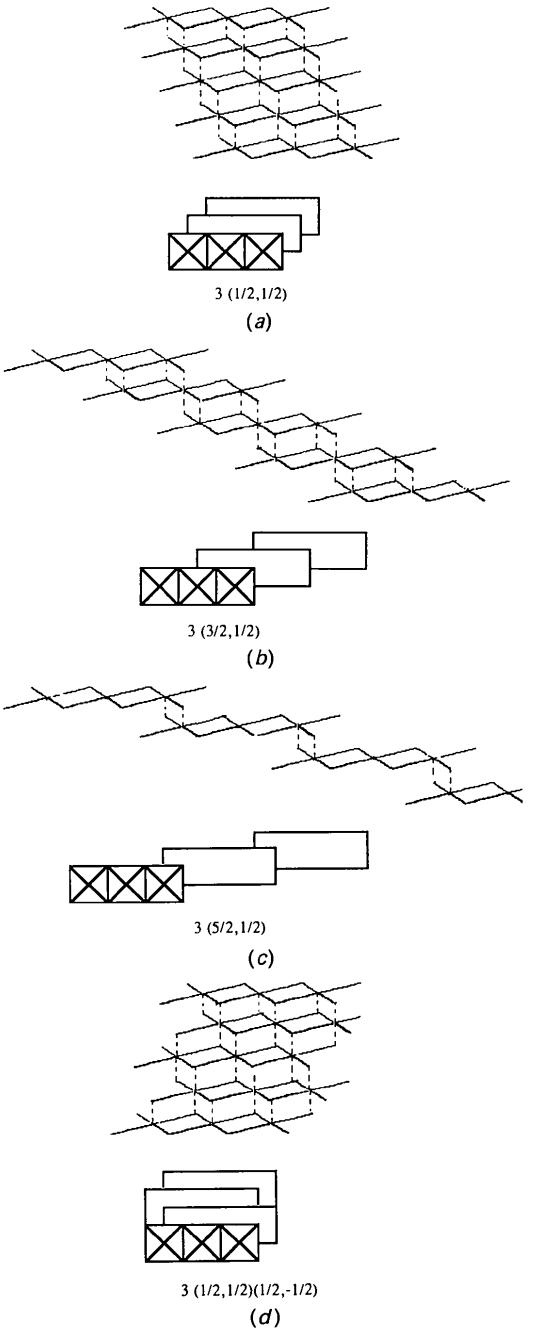

Fig. 4. (*a*)–(*d*) Envelope diagrams representing stacking patterns of compounds of stoichiometry $A_2Cu_3X_8$, ACu_3X_7L and $Cu_3X_6L_2$. The Geiser notation for the stacking pattern is also given.

Removal of Cu^{II} *ions coupled with stacking faults*

The strain introduced by electrostatic repulsion between halide ions upon removal of individual Cu^{II} ions can be alleviated by the introduction of stacking faults. When this occurs, interdigitated stacks of oligomers are formed, as illustrated by the stacking pattern in Fig. 7.* This is observed in several salts

* It is possible to define several possible stacks within this planar aggregation of oligomers. This introduces some ambiguity into the stacking-pattern notation. The problem is resolved by defining two different stacking patterns that uniquely define the layer structure. In the stacking-pattern symbol, the two definitive patterns are distinguished from one another by enclosing them in brackets.

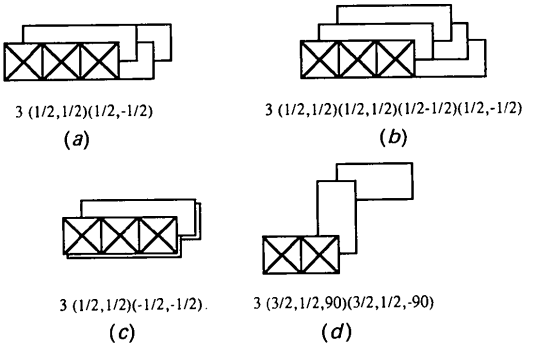

Fig. 5. (*a*)–(*d*) Envelope diagrams and Geiser notation for stacking patterns with stacking faults corresponding to a shift of a row of metal ions from sites between one pair of layers to sites between the adjacent pair of layers.

(Willett & Rundle, 1964; Bond, 1990). Energetically, this is favorable since it allows each Cu^{II} ion to form two semicoordinate bonds.

Insertion of ligands between chains

A final mechanism for the attainment of charge balance upon addition of a cation into the structure would be the insertion of halide ions between adjacent chains in the layers. No such structures are currently known, although, when viewed from this perspective, the structures $Me_4PCu_2Cl_5$ (Haije, Dobbelaar & Maaskant, 1986) and $Me_4AsCu_2Cl_5$ (Murray & Willett, 1993) come close to attaining this arrangement. However, the square-pyramidal coordination spheres about the Cu^{II} ions are arranged in an antiferrodistortive fashion within each chain, so the close analogy to the ferrodistortive $CuCl_2$ structure is lost. Insertion of neutral ligands, which occurs in several compounds, leads to a breakdown of the layer structure (see Willett, 1988).

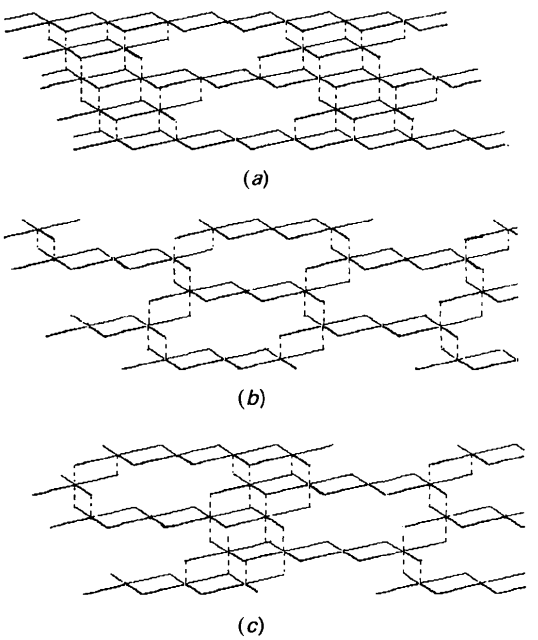

Fig. 6. Illustrations of the structures for (*a*) the title compound, $[(C_2H_5)_3NCH_3]Cu_3Cl_7$, and the hypothetical (*b*) $A_2Cu_3X_8$ and (*c*) $A_2Cu_4X_{10}$ compounds formed by the removal of $Cu_2Cl_2^{2+}$ fragments from the parent compound.

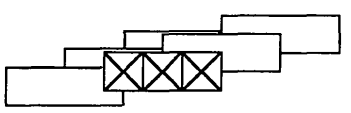

Fig. 7. Envelope diagram and Geiser notation for the stacking pattern of oligomers formed by the removal of Cu^{II} ions and the introduction of stacking faults.

Concluding remarks

The crystal structure of the title compound, $(Et_3NMe)Cu_3Cl_7$, is readily described in terms of the parent $CuCl_2$ structure. The basic feature is the replacement of $Cu_2Cl_2^{2+}$ units in alternate chains by pairs of the organic cations. This represents a new mechanism for modification of the $CuCl_2$ structure.

The ferrodistortive $CuCl_2$ structure is shown to be surprisingly resistant to structural modification, with the basic features retained in a large number of structural variations. The most common modification is simple termination of the chains by additional halide ions and/or ligands. Addition of stacking faults, coupled with chain termination or $Cu_2Cl_2^{2+}$ unit replacement, leads to additional structural modifications. A final mechanism, insertion of halide ions or ligands between chains, leads to breakdown of the structure in all cases observed to date.

Research supported in part by NSF grant DMR-8893382. Acknowledgement is made to The Boeing Company and to the NSF, through grant CHE-8408407, for the establishment of the X-ray diffraction facility.

References

BALZ, D. (1953). *Naturwissenschaften*, **40**, 241.
BOND, M. R. (1990). PhD thesis, Washington State Univ., Pullman, WA 99164, USA.
BOND, M. R., PLACE, H., WILLETT, R. D., LIU, Y., GRIGEREIT, T., DRUMHELLER, J. & TUTHILL, G. (1993). In preparation.
BOND, M. R. & WILLETT, R. D. (1989). *Inorg. Chem.* **28**, 3267–3269.
CAMPANA, C. F., SHEPARD, D. F. & LITCHMAN, W. M. (1981). *Inorg. Chem.* **20**, 4039–4044.
GEISER, U., WILLETT, R. D., LINDBECK, M. & EMERSON, K. (1986). *J. Am. Chem. Soc.* **108**, 1173–1179.
GOMES-CUEVAS, A., TELLO, M. J., FERNANDEZ, J., LOPEZ-ECHARRI, A., HERREROS, J. & COUZI, M. (1983). *J. Phys. C*, **16**, 473–485.
HAIJE, W. G., DOBBELAAR, J. A. L. & MAASKANT, W. J. A. (1986). *Acta Cryst.* C**42**, 1485–1487.
HATFIELD, W. E. (1985). *Magneto-Structural Correlations in Exchange Coupled Systems*, edited by R. D. WILLETT, D. GATTESCHI & O. KAHN, pp. 555–602. Dordrecht: Reidel.
MANFREDINI, T., PELLACANI, G. C., BONAMARTINI-CORRADI, A., BATTAGLIA, L. P., GUARINI, G. G. T., GIUSTI, J. G., PON, G., WILLETT, R. D. & WEST, D. X. (1990). *Inorg. Chem.* **29**, 2221–2228.
MURRAY, K. & WILLETT, R. D. (1993). *Acta Cryst.* Submitted.
SHELDRICK, G. M. (1985). *SHELXTL*. Version 5.1. Nicolet Analytical Instruments, Madison, WI, USA.
TANAKA, H., IIO, K. & NAGATA, K. (1985). *J. Phys. Soc. Jpn*, **54**, 4345–4358.
TISCHENKO, G. N. (1955). *Tr. Inst. Kristallogr. Akad. Nauk SSSR*, **11**, 93–96.
WELLS, A. F. (1947). *J. Chem. Soc.* pp. 1670–1675.
WELLS, A. F. (1984). *Structural Inorganic Chemistry*, 5th ed. Oxford: Clarendon Press.
WILLETT, R. D. (1964). *J. Chem. Phys.* **40**, 838–847.
WILLETT, R. D. (1966). *J. Chem. Phys.* **44**, 39–42.

WILLETT, R. D. (1988). *Acta Cryst.* B44, 503–508.
WILLETT, R. D., BOND, M. R., HAIJE, W. E., SOONIEUS, O. P. M. & MAASKANT, W. J. A. (1988). *Inorg. Chem.* 27, 614–620.
WILLETT, R. D., BOND, M. R. & PON, G. (1990). *Inorg. Chem.* 29, 4160–4162.
WILLETT, R. D. & GEISER, U. (1986). *Inorg. Chem.* 25, 4558–4561.
WILLETT, R. D., GRIGEREIT, T., HALVORSON, K. & SCOTT, B. (1987). *Indian Acad. Sci.* 98, 147–160.
WILLETT, R. D., PLACE, H. & MIDDLETON, M. (1988). *J. Am. Chem. Soc.* 110, 8639–8650.
WILLETT, R. D. & RUNDLE, R. E. (1964). *J. Chem. Phys.* 40, 838–847.

Acta Cryst. (1993). B49, 289–303

Structures of Hexakis(1-propyltetrazole)iron(II) Bis(tetrafluoroborate), $[Fe(CHN_4C_3H_7)_6](BF_4)_2$, Hexakis(1-methyltetrazole)iron(II) Bis(tetrafluoroborate), $[Fe(CHN_4CH_3)_6](BF_4)_2$, and the Analogous Perchlorates. Their Relation to Spin Crossover Behaviour and Comparison of Debye–Waller Factors from Structure Determination and Mössbauer Spectroscopy

BY LEONORE WIEHL

Mineralogisches Institut der Universität Bonn, Poppelsdorfer Schloß, 5300 Bonn 1, Germany

(*Received* 14 *December* 1991; *accepted* 24 *August* 1992)

Abstract

Single-crystal structure determinations of the spin crossover compounds $[Fe(ptz)_6]X_2$ and $[Fe(mtz)_6]X_2$ (ptz = $C_3H_7N_4CH$, mtz = CH_3N_4CH, $X = BF_4$, ClO_4) have been performed at different temperatures. The temperature dependence of the lattice constants was measured for the two mtz compounds between 300 and 110 K. The two different structure types for the ptz and mtz compounds are compared and discussed in relation to the physical properties associated with the temperature-induced and light-induced spin transitions. In particular, the atomic displacement parameters for the two inequivalent Fe complexes in the mtz structure were found to be significantly different. They are in good accordance with the vibrational amplitudes derived from the Debye–Waller factors measured by Mössbauer spectroscopy. Crystal data, measured with Mo $K\alpha$ radiation, $\lambda = 0.71069$ Å: (*S*1) $[Fe(ptz)_6](ClO_4)_2$ at 299 K: $M_r = 927.6$, $R\bar{3}$ ($Z = 3$), D_m (295 K) = 1.33, $D_x = 1.333$ Mg m^{-3}, $a = 10.804$ (3), $c = 34.296$ (5) Å, $V = 3467$ (1) Å^3, $F(000) = 1446$, $\mu = 0.461$ mm^{-1}, $R = 0.115$ (1965 unique reflections), isostructural to (*S*2). (*S*2) $[Fe(ptz)_6](BF_4)_2$ at 297, 250 and 195 K: $M_r = 902.3$, $R\bar{3}$ ($Z = 3$), D_m (295 K) = 1.32, $D_x = 1.312$ Mg m^{-3}, $a = 10.833$ (2), $c = 33.704$ (6) Å, $V = 3425$ (1) Å^3 at 297 K, $a = 10.857$ (3), $c = 33.053$ (13) Å, $V = 3374$ Å^3 at 250 K and $a = 10.890$ (2), $c = 32.330$ (10) Å, $V = 3320$ (1) Å^3 at 195 K; $F(000) = 1398$; $\mu = 0.368$ mm^{-1} (297 K), 0.373 mm^{-1} (250 K) and 0.380 mm^{-1} (195 K); $R = 0.125$ (2058 unique reflections) at 297 K, $R = 0.114$ (1799 unique reflections) at 250 K and $R = 0.077$ (1695 unique reflections) at 195 K. (*S*3) $[Fe(mtz)_6](ClO_4)_2$ at 298 K: $M_r = 759.2$, $P2_1/n$ ($Z = 4$), $D_m = 1.55$, $D_x = 1.551$ Mg m^{-3}, $a = 18.270$ (4), $b = 10.367$ (2), $c = 18.674$ (5) Å, $\beta = 113.16$ (2)°, $V = 3252$ (1) Å^3, $F(000) = 1544$, $\mu = 0.647$ mm^{-1}, $R = 0.083$ (4529 unique reflections), isostructural to (*S*4). (*S*4) $[Fe(mtz)_6](BF_4)_2$ at 157 and 113 K: $M_r = 733.9$, $P2_1/n$ ($Z = 4$), $D_m = 1.53$, $D_x = 1.524$ Mg m^{-3} at 295 K; $a = 17.778$ (6), $b = 10.215$ (2), $c = 18.625$ (6) Å, $\beta = 114.03$ (2)°, $V = 3089$ (2) Å^3 at 157 K and $a = 17.673$ (7), $b = 10.178$ (5), $c = 18.648$ (8) Å, $\beta = 114.27$ (3)°, $V = 3058$ (2) Å^3 at 113 K; $F(000) = 1480$; $\mu = 0.535$ mm^{-1} (157 K) and 0.540 mm^{-1} (113 K); $R = 0.090$ (4485 unique reflections) at 157 K and $R = 0.074$ (4625 unique reflections) at 113 K.

Introduction

The tetrazole compounds of type $[Fe(R\text{-tz})_6]X_2$ (*R*-tz = 1-alkyltetrazole, $X = BF_4$, ClO_4, PF_6, CF_3SO_3) belong to the large group of octahedrally coordinated Fe^{2+} spin crossover compounds, which undergo a transition from the high-spin (HS) state ($^5T_2$) to the low-spin (LS) state ($^1A_1$) on cooling. HS $\rightarrow$LS transitions are accompanied by a contraction of the Fe—ligand bond distances of up to 0.2 Å (see review of X-ray structures: König, 1987), leading to elastic interactions between large HS and small LS molecules in the transition region (Spiering, Meissner, Köppen, Müller & Gütlich, 1982; Adler,

0108-7681/93/020289-15$06.00